AD-A091 719 MASSACHUSETTS INST OF TECH CAMBRIDGE AEROPHYSICS LAB F/G 4/1
WIND TUNNEL TESTS OF A GERDIEN CAPACITOR VEHICLE COMBINATION,(U)
MAY 80 C W HALDEMAN F19628-79-C-0059
UNCLASSIFIED MIT-TR-206 AFGL-TR-80-0179 NL

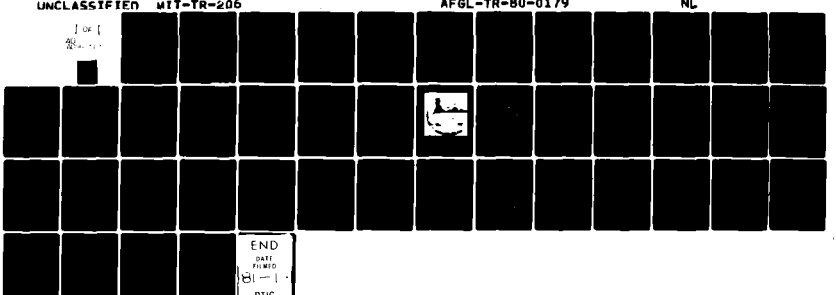

END
DATE FILMED
81-1
DTIC

LEVEL II

(12) 43

(18) AFGL (19) TR-80-0179

(6) WIND TUNNEL TESTS OF A GERDIEN CAPACITOR VEHICLE COMBINATION

(7) Charles W. Haldeman

Massachusetts Institute of Technology
Department of Aeronautics and Astronautics
Aerophysics Laboratory
Cambridge, Massachusetts 02139

(11) May 80

(12) 43

(14) MIT-TR-206

(9) Final Report.
1 Feb 79 — 30 Apr 80

(15) F19628-79-C-0059

Approved for public release; distribution unlimited.

(16) 2319 (17) G3

Air Force Geophysics Laboratory
Air Force Systems Command
United States Air Force
Hanscom AFB, Massachusetts 01731

009200

Unclassified

SECURITY CLASSIFICATION OF THIS PAGE (When Data Entered)

REPORT DOCUMENTATION PAGE	READ INSTRUCTIONS BEFORE COMPLETING FORM
1. REPORT NUMBER: AFGL-TR-80-0179 / 2. GOVT ACCESSION NO.: AD-A091719	3. RECIPIENT'S CATALOG NUMBER:
4. TITLE (and Subtitle): WIND TUNNEL TESTS OF A GERDIEN CAPACITOR VEHICLE COMBINATION	5. TYPE OF REPORT & PERIOD COVERED: Final 2/1/79 - 4/30/80
	6. PERFORMING ORG. REPORT NUMBER: M.I.T. TR 206
7. AUTHOR(s): Charles W. Haldeman	8. CONTRACT OR GRANT NUMBER(s): F19628-79-C-0059
9. PERFORMING ORGANIZATION NAME AND ADDRESS: Massachusetts Institute of Technology, Aerophysics Laboratory, Cambridge, Massachusetts 02139	10. PROGRAM ELEMENT, PROJECT, TASK AREA & WORK UNIT NUMBERS: 61102F, 2310G3AP
11. CONTROLLING OFFICE NAME AND ADDRESS: Air Force Geophysics Laboratory, Hanscom AFB, Massachusetts 01731, Monitor/Edmund A. Murphy/LKD	12. REPORT DATE: May, 1980
	13. NUMBER OF PAGES: 42
14. MONITORING AGENCY NAME & ADDRESS (if different from Controlling Office)	15. SECURITY CLASS. (of this report): Unclassified
	15a. DECLASSIFICATION/DOWNGRADING SCHEDULE

16. DISTRIBUTION STATEMENT (of this Report)

Approved for public release; distribution unlimited

17. DISTRIBUTION STATEMENT (of the abstract entered in Block 20, if different from Report)

18. SUPPLEMENTARY NOTES

19. KEY WORDS (Continue on reverse side if necessary and identify by block number)

Ground testing
Gerdien capacitor
Atmospheric probe
Supersonic flow

20. ABSTRACT (Continue on reverse side if necessary and identify by block number)

Wind tunnel tests at MIT and AEDC of a rocket borne upper atmospheric probe for measuring atmospheric charge density are reported. The Gerdien capacitor probe consists of a short section of a coaxial capacitor. This is mounted on pylons from a model of the Tomahawk vehicle. Results are reported for the Mach number range 2 to 4 and altitude range 38 to 95 Km and compared with previous data. Over this range the ratio of mass flow through the probe to mass flow in an equal cross section of the free stream

DD FORM 1 JAN 73 1473 EDITION OF 1 NOV 65 IS OBSOLETE
S/N 0102-014-6601

Unclassified

SECURITY CLASSIFICATION OF THIS PAGE (When Data Entered)

ranged from .2 to .80. Reported measurements extend the range of altitude and Mach number for which data is available. Best correlation of mass capture efficiency is obtained as a function of the viscous interaction parameter $M\sqrt{Re_\infty}$. In terms of this parameter capture efficiency exhibits a minimum of .2 at 50; rising to 0.5 at 15 and .8 at 1000.

PREFACE

This Final Report on Contract F19628-79-C-0059 with Air Force Geophysics Laboratory describes wind tunnel test results for vehicle-mounted Gerdien capacitor probes conducted between 1 February 1979 and 30 April 1980 under the technical cognizance of Mr. Edmund A. Murphy, Contract Monitor. Earlier work on this subject was performed previously under Contract F19628-76-C-0185 and reported in AFGL-TR-79-0009.

The author wishes to acknowledge the assistance of Mr. Robert E. Alt, the Project Engineer at AEDC and other ARO personnel who performed the tests at the Arnold Center.

Professional personnel who contributed to this research are Professor Morton Finston and Dr. Charles W. Haldeman.

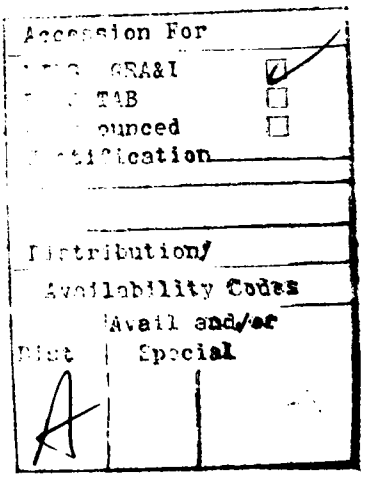

TABLE OF CONTENTS

INTRODUCTION

Supersonic flight through the atmosphere is always accompanied by the formation of a shock wave near the nose of the vehicle. When the body is slender and sharp nosed, this wave is attached to the point at an oblique angle and propagates away from and behind the vehicle. In cases where the body is blunt or the nose is rounded, the shock wave is displaced from the nose (detached).

Under Contract F19628-76-C-0185 the M.I.T. Aerophysics Laboratory conducted a several part study of the shock position on a conical skimmer. A series of wind tunnel tests using a one-tenth scale model has been completed and response of the shock position to Mach number and angle of attack changes was measured using the 18 x 24 inch supersonic wind tunnel at equivalent altitude from 27.5 to 65 Km. Response of the shock wave position to viscous intermolecular effects at higher altitude was assessed from both the full-scale tests at AEDC and a brief test using the small (3-inch nozzle diameter) high altitude test apparatus and a nitrogen arc jet. All results have been reported in AFGL-TR-77-0210 (1).

In addition to the mass spectrometer probe the Tomahawk vehicle will carry a Gerdien capacitor for the measurement of atmospheric charge density. Because this instrument cannot be deployed at a great enough distance from the vehicle to place it ahead of the bow shock, as determined from the recent M.I.T. tests (2), it is necessary to calibrate it in the presence of the vehicle. Preliminary wind tunnel tests of a one-tenth scale and one-quarter scale Gerdien capacitor have been conducted and reported (2).

During these tests, using the one-quarter scale model, impact pressure surveys were made behind the Gerdien to provide calibration of the Gerdien. The results indicate that the flow through the Gerdien is complex and that disgorgement is a gradual process (2). This Final Report presents additional data from current tests using both the M.I.T. Wind Tunnel and the 10v space chamber facility at AEDC. Data is reported for altitudes from 38 to 95 Km at Mach numbers from 2 to 4.

TEST GOALS

The purpose of the test program was to determine the mass capture efficiency of the Gerdien as a function of Mach number and altitude. This capture efficiency is needed in order to relate the charge collected by the Gerdien to the

charge present in the undisturbed atmosphere. In planning the calibration tests reported it was assumed that the charged particles being sampled in the atmosphere were completely coupled to the neutral background gas; i.e., whatever deviation from free stream sampling existed could be determined from the behavior of the neutral gas. The required data is then a measurement of the mass flow through the Gerdien compared to the mass flow far away from the vehicle. These flows are not the same for the following reasons:

1. The Gerdien is deployed inside the vehicle bow shock wave. Therefore, the flow ahead of the Gerdien has traversed compression through this shock wave; expansion along the short cylindrical section (Figure 1); compression in another shock ahead of the conical frustrum; and final expansion along the cylindrical body. These regimes are clearly visible in Figures 4 and 9 of Reference 2 and Figure 3 of this report.

2. Simple inviscid blockage of the Gerdien below a local Mach number of 1.28 due to shock wave detachment from the Gerdien conical center body.

3. Viscous growth of boundary layers on center body, inside bore and support rods which decrease the available flow area and raise the Mach number for detachment well above effect (2).

4. At low densities collisions with the condenser leading edge and center body scatter particles forward to produce a higher density lower velocity gas cloud ahead of the Gerdien. At extremely low density there are few collisions and this effect loses importance.

In the tests reported here the aggregate effect of these influences has been determined by making surveys of the flow as close as possible behind the Gerdien.

Tests were carried out using the M.I.T. Supersonic Wind Tunnel at equivalent altitudes from 38 to 49 Km and at AEDC from 81 to 95 Km. Combined with the previous data (2) from 29 to 44 Km this provides information from 29 to 95 Km over the Mach number range 2 to 3.7.

TEST MODEL

The test model used was the one-quarter scale model of the Tomahawk vehicle and Gerdien from previous tests (2). It is shown in Figure 1. This model was also shown in Figure 1 of Reference 2. However, the position of the Gerdien in Reference 2 is in error. All reported data was taken with the Gerdien at the 13.4 inch station shown in this report. Tests of the one-tenth scale model (2) showed that the 13.4 inch station provided a wider range of operation with an attached shock.

Details of the Gerdien construction are shown in Figure 2 (also from Reference 2). Paths of the surveys at AEDC have been added to this figure.

Flow properties behind the Gerdien were determined in the M.I.T. tests by making impact pressure and static pressure surveys along a line in the Gerdien and support Pylon center plane one-half inch downstream of the Gerdien. The impact probe assembly was similar to that used previously (2) but a static probe was added parallel to and below the impact tube. The static pressure probe was a .112 inch base diameter 2.5^{o} half angle sharp cone with four pressure taps one-half inch back along the cone. The probe and Gerdien are shown in Figure 3, a Schlieren photograph of Run 5.

By using this double probe plots of both impact pressure and static pressure were made with one traverse behind the Gerdien by using two plotters. In reducing the data the .939 inch offset between probes was subtracted so static and impact pressures were compared at the same point.

Impact pressure was measured using a Statham 2.5 psia pressure transducer located inside the model. Static pressure measurements used a similar 1 psia transducer.

For the AEDC tests the probe and model mounting yokes were removed and the holes were fitted with smooth aluminum plugs. The Gerdien was also modified by replacing the leading and trailing edges of the outer cylinder with copper while maintaining the dimensions of Figure 2. This was necessary to ensure that impingement of the electron beam used for diagnostics did not damage the model. Details of the AEDC set-up may be found in Reference 3.

M.I.T. TEST RESULTS

Results of the current one-quarter scale tests extend previous results to higher altitudes and a wider range of Mach numbers and the use of a movable static pressure probe provided more accurate Mach number measurements. This indicated that the Mach number behind the Gerdien was lower than reported earlier (2) and resulted in a general lowering of the measured capture efficiencies. A sample comparison of the two sets of measurements for the same flow conditions are shown in Figure 4. The lower values found for Mach number using the static survey are evident in this figure. For this reason the earlier data has not been weighted heavily in drawing the curve of Figure 7.

The complex character of the flow found at first (2) was confirmed and this complexity combined with the averaging and integration processes used to obtain Gerdien mass flow are responsible for the high scatter in both new data and old data. A summary of the test conditions is given in Table 1. A typical Schlieren photograph is shown in Figure 3.

DATA REDUCTION

Impact and static transducer data were reduced to pressures using the transducer sensitivity and zero obtained before each days operation and these pressures were used to find Mach number using the compressible flow function tables of Reference 4. Static temperature and sound speed were then calculated from recorded tunnel stagnation temperature, Mach number just determined, and tables (4). Condenser mass flows were averaged over the condenser by choosing 10 zones and multiplying velocity by density by area for each zone and then summing. The condenser wake was divided into five annular regions. The 90 degrees behind the struts formed five zones and the remaining 270 formed the other five zones. The radius of the outer zone was selected to match the observed wake profile. This was about 1.2 inches outside diameter. This method was chosen because it seemed a more realistic match to the observed symmetry than the trapezoidal zones used in Reference 2.

Reynolds numbers were determined from Figures 5 and 6 for free flight of a 12" diameter vehicle. These figures appeared in Reference 2 with axes incorrectly labeled. They have been corrected here. All tabulated data in Reference 2 are correct.

AEDC TEST RESULTS

Tests at AEDC were carried out in test chamber 10-V and are described in Reference 3. These differed somewhat from those at MIT in that at the higher altitudes of these tests pitot-static probes are subject to large errors so the basic probing technique used was spectrographic. An electron beam was used to produce flow luminessence, which provided a determination of flow density and temperature from observations of the nitrogen rotational fine structure. Temperature and density profiles both ahead of and behind the Gerdien were obtained by moving the model in the wind stream with respect to the electron beam and optical equipment. These are presented in Reference 3. Temperature and density were converted to Mach number, velocity and mass flux by computing local sound speed from local temperature, $a=20.38\ \sqrt{T(^{o}K)}$ m/sec and applying conservation of energy to the flow using free stream as a reference. (Because of shock waves and viscous effects, momentum is not conserved.)

This yields

$$U = \left(U_{\infty}^{2} - (T-T_{\infty})\ \ 2.08 \times 10^{3}\right)^{1/2}$$

for U, the magnitude of the local velocity vector, in terms of the temperature in ^{o}K.

Plots of $\rho.U$ and M vs distance outward from the wall are given in the Appendix as is the tabulated AEDC data with values for U, M and $\rho.U$.

The capture efficiency = $\frac{\dot{m}\ \text{Gerdien}}{\dot{m}\ \text{free stream}}$ and other summary data from the AEDC test are given in Table 1. Free stream conditions are given in Table 2. Details of the M.I.T. test conditions are listed in Table 1a. The data is summarized in Figures 7 and 8. Note that the data from Reference 2 which was less accurate, as discussed above (large open symbols), was not weighted heavily in drawing the curve of Figure 7. The plot against viscous interaction parameter $M\sqrt{Re}$ (Figure 8) cuts down the scatter somewhat over the straight altitude plot (Figure 7). However, the large scatter prevents a precise determination of the calibration curve. Data from Reference 2, Table 3, is also included in these figures.

DISCUSSION OF RESULTS

The results of the two series of tests at M.I.T. and one series at AEDC indicate that the Gerdien capture efficiency on the Tomahawk vehicle varies between .8 and .2, depending on Mach number and altitude. As pointed out previously (2), the flow pattern is very complex and at high altitudes (AEDC) a high temperature, high density, subsonic region builds up ahead of the Gerdien and its supports. A large fraction of the incident flow spills around the Gerdien under these conditions.

At 95 Km near the free molecule flow regime the upstream disturbance disappears and the capture efficiency returns to a high value.

In Figure 9 the test points are plotted in the Mach number altitude plane to show the location of the detachment boundary. This is mainly of academic interest because response of the Gerdien to detachment is gradual and the data of Figures 7 or 8 should be used to reduce individual flight data because of the wide range over which the capture efficiency changes.

The procedure recommended for reducing flight data is to use the curve of Figure 8 to determine capture efficiency for various points on the trajectory for which M and Re have been computed. This appears preferable to use of Figure 7 because of its larger scatter.

It should be remembered in reducing flight data that any change in Gerdien geometry, location or vehicle nose shape will change the capture efficiency, particularly the low altitude limit. Thus the results should not be used for other geometries without experimental confirmation.

REFERENCES

1. Haldeman, C W, R A Kraemer and B Ziph, "Wind Tunnel Tests of the Upstream Influence of a Conical Mass Spectrometer Probe", AFGL-TR-77-0210, MIT Aerophysics Lab TR 197, Sept., 1977.

2. Haldeman, C W, R H Bush and S W Prey, "Some Effects of Vehicle Flow Field on the Capture Efficiency of a Gerdien Capacitor Atmospheric Probe", AFGL-TR-79-0009, MIT Aerophysics Lab TR 204, Dec., 1978.

3. Alt, R E, L L Price, D H Campbell, W B Stephenson and H M Powell, "Temperature and Density Measurements Near a 1/4 Scale Model Upper Atmospheric Probe at Mach Number 3.5", AEDC-TSR-80-V19 and Test Data Package, April, 1980.

4. NACA Report 1135, "Equations, Tables and Charts for Compressible Flow, Ames Research Staff, 1953.

Table 1

Data from MIT and AEDC Tests

Run	M	Nozzle	Re		$M\sqrt{Re}$	Mass Flow Ratio	Altitude Km	Shock State*
					MIT Test Data			
1	1.90	2	.107	+6	621	.615	35	A
2	1.89	2	.0428	+6	391	.627	41	iD
3	1.95	2	.04118	+6	396	.563	41	D
4	1.93	2	.0182	+6	260	.548	47	D
5	2.45	2.5	.075	+6	671	.626	38.5	A
5a	2.46	2.5	.075	+6	674	.634	38.5	A
7	2.45	2.5	.05	+6	548	.492	41.5	A
8	2.43	2.5	.03	+6	421	.58	45	A
9	2.11	2.5	.0162	+6	266	.497	48	D
10	2.79	3	.0619	+6	694	.597	40	A
11	2.6	3	.030	+6	450	.441	45	A
12	2.38	3	.0173	+6	313	.642	49	A
14	3.44	4	.0506	+6	774	.376	43.5	A
15	3.02	4	.028	+6	505	.417	47	A
					AEDC Test Data			
A	3.76		454		80	.191	81	D
B	3.74		245		58	.211	84.5	D
C	3.54		90		33.6	.197	89	D
D	3.42		19.6		15	.515	95	A

*A = attached
D = detached
iD = incipient detachment

Table 1a

MIT Wind Tunnel Run Conditions

Run Number	M Nominal	P_o (psia)	P_s (torr)	T_o °F	Photo Number
1	2	1.5	11.4	67	65624
2	2	.6	4.7	66	65625-7
3	2	.6	4.37	81	65628
4	2	.27	1.99	81	65636
5	2.5	1.5	4.87	96	65637-9
6	2.5	.6	Flow Breakdown		65640-3
7	2.5	1	3.27	95	65644-7
8	2.5	.6	2.04	95	65648-53
9	2.5	.27	1.56	90	65654-7
10	3.0	1.5	2.9	73	65658-60
11	3.0	.6	1.55	75	65661-4
12	3	.33	1.2	74	65665-8
-					
14	4	1.5	1.1	74.5	65669-72
15	4	.7	.95	77	65673-6

Table 2

AEDC Free Stream Conditions

Condition	P_{T_1} (mtorr)	T_{T_1} (^{o}K)	M	Alt(Km)	Re	λcm	ρu x 10^{-18} (N/cm^2/sec)
A	900	290	3.76	81	454	.08	68.2
B	450	286	3.74	84.5	245	.15	35.1
C	150	283	3.54	89	90	.38	13.65
D	150	863	3.42	95	19.6	1.8	6.87

*Note annular gap in Gerdien model was .85 cm.

Table 3

One-Quarter Scale Model Reference 2 Data

M	α	Photo No.	P_o	T_o	$Re_D 10^6$	Alt(Km)	$\frac{\dot{m}}{\dot{m}_{f.s.}}$	$M\sqrt{Re}$
2.25	0	65526-528	5	110	.269	29.6	.801	1166
2.25	0	538	3	110	.161	32.9	.784	903
2.25	0	545	1.5	105	.0806	37.5	.752	639
2.25	0	559	.63	108	.0339	43.8	.739	414
2.0	0		5.0	110	.3025	28.9	.698	1100
2.0	0	590	3.0	110	.1815	31.4	.758	852
2.0	0	597	1.5	110	.0908	35.9	.734	603
2.0	0	604	.64	110	.0387	42.3	.689	393

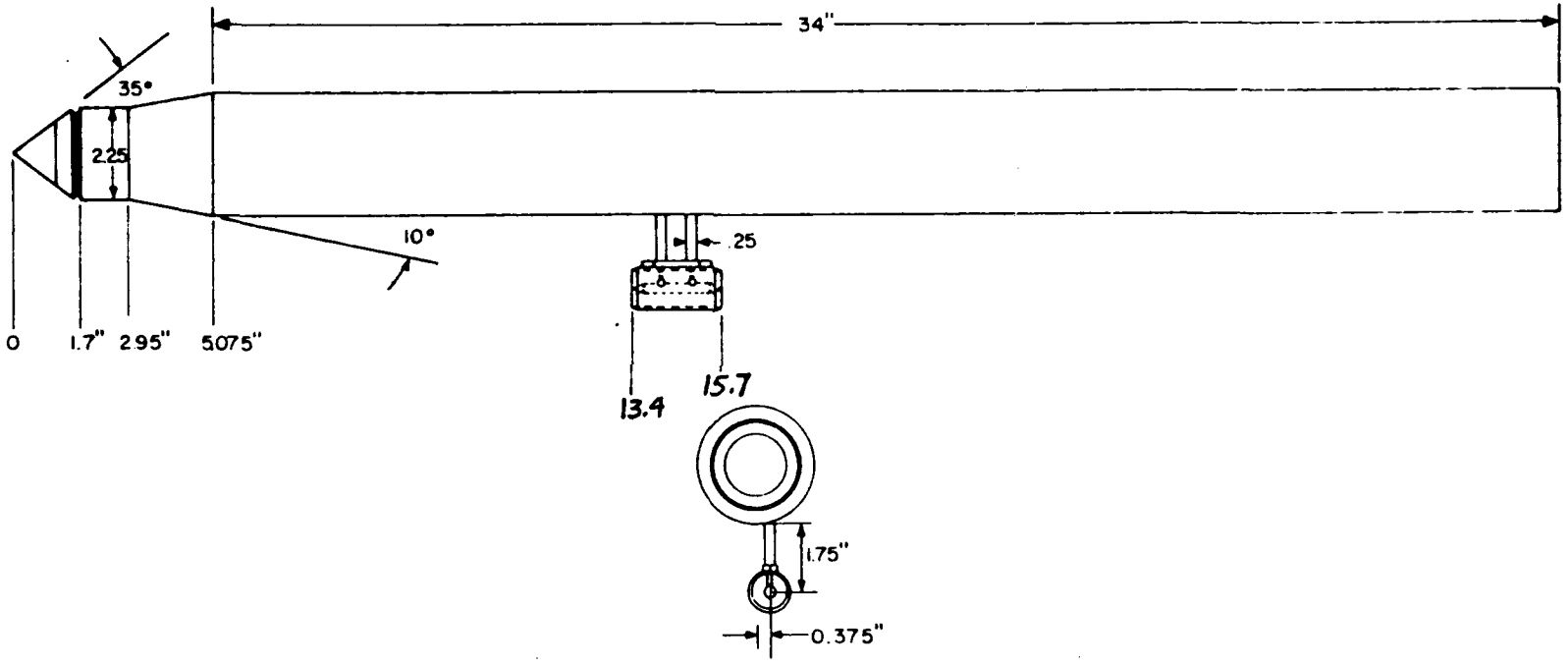

Figure 1. 1/4 Scale Model of Gerdien Capacitor and Tomahawk Vehicle

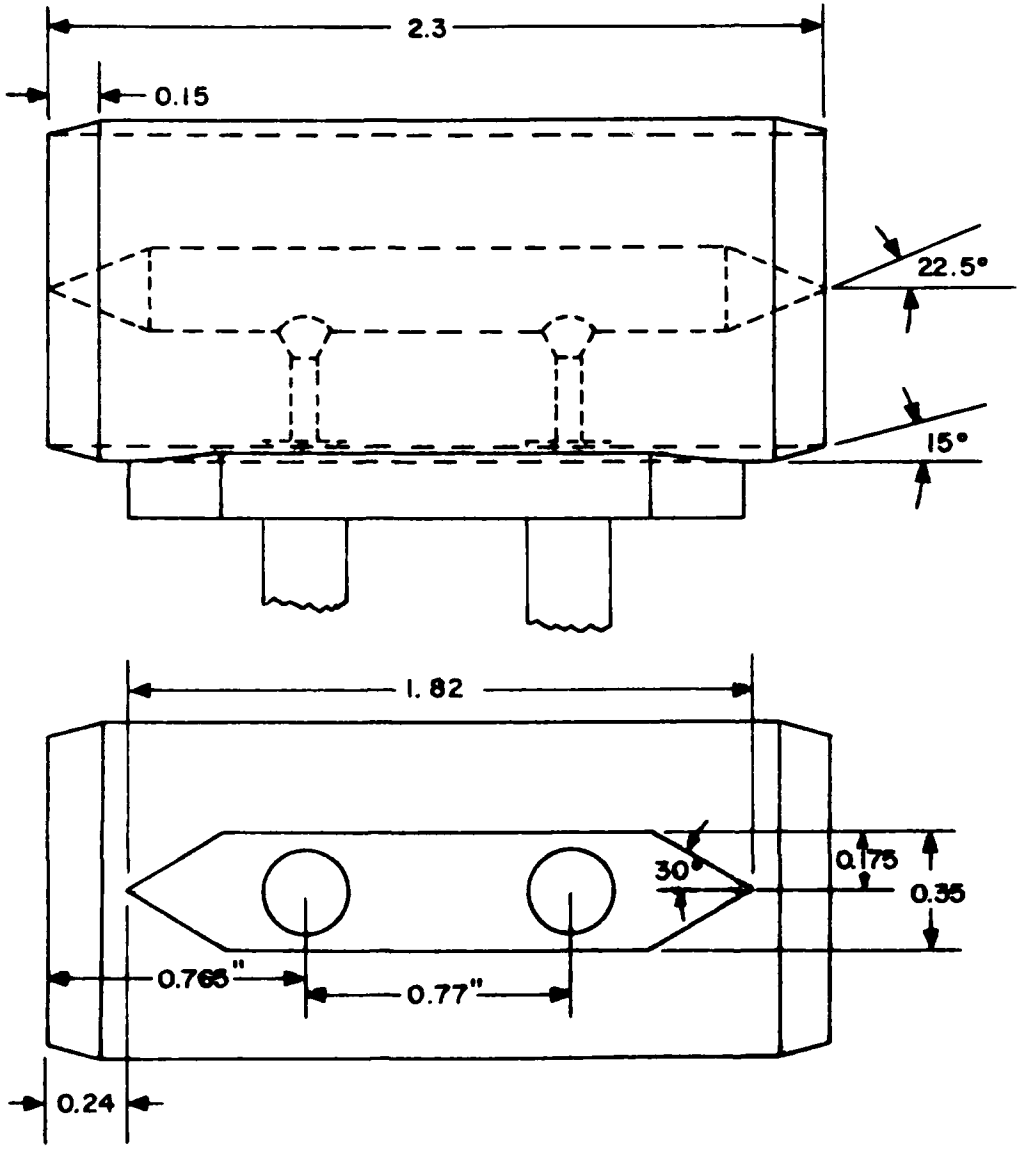

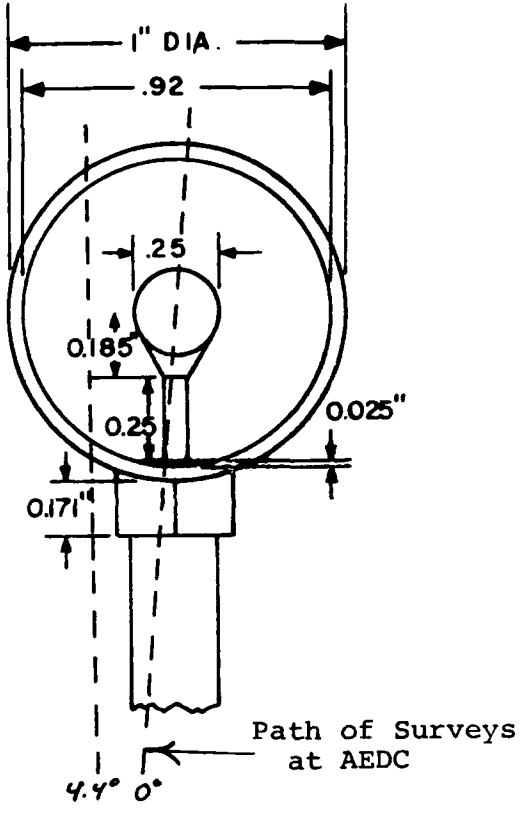

Figure 2.

Gerdien capacitor detail

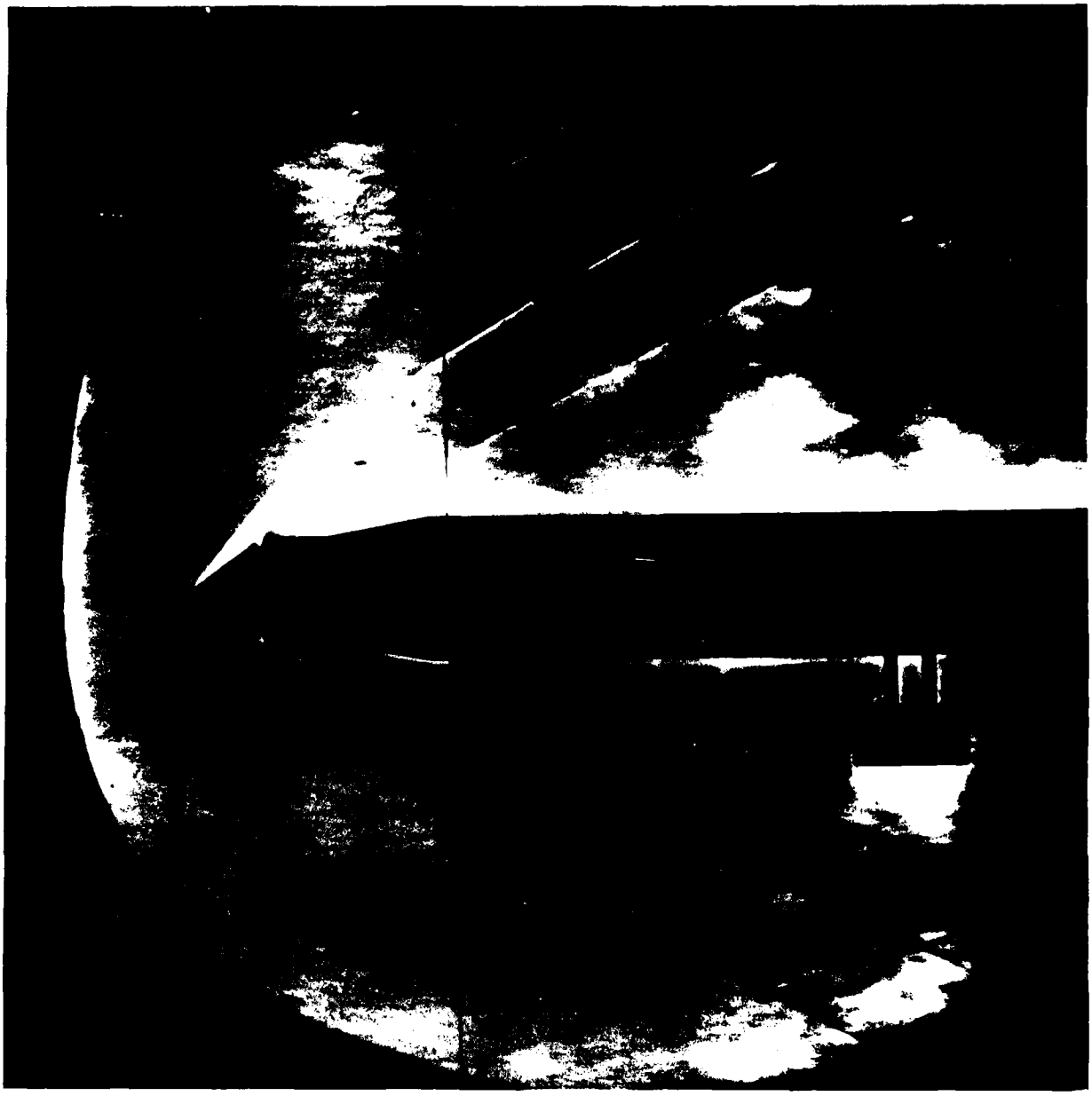

Figure 3. Typical Schlieren Photograph of Model and Gerdien in MIT Tunnel

Run 5, M=2.5, P_o=1.5 psia, 38.5 Km altitude

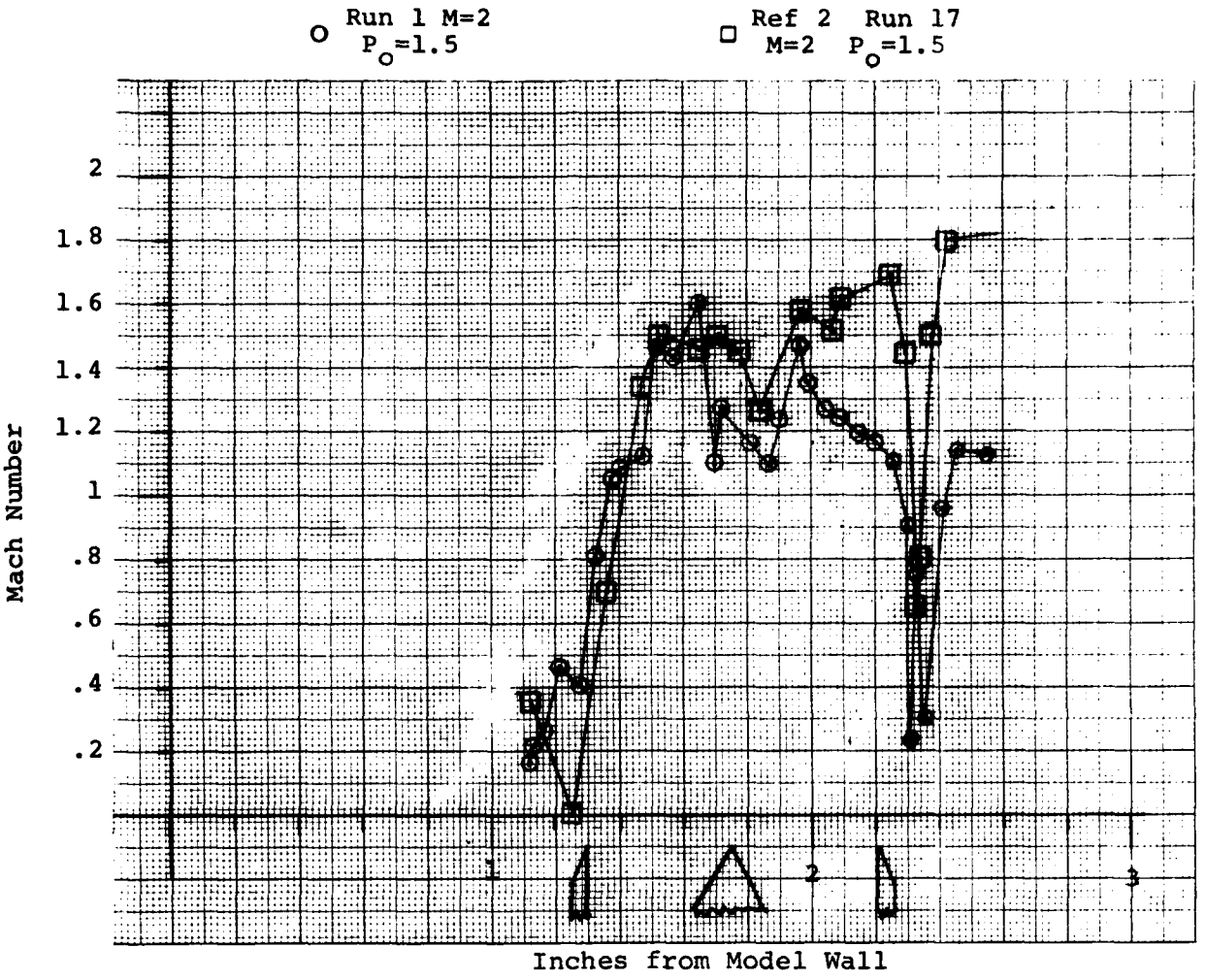

Figure 4. Mach Number Profiles comparing Mach Number computed from Static Pressure Survey (Run 1) with Method of Reference 2, assuming Constant Static Pressure

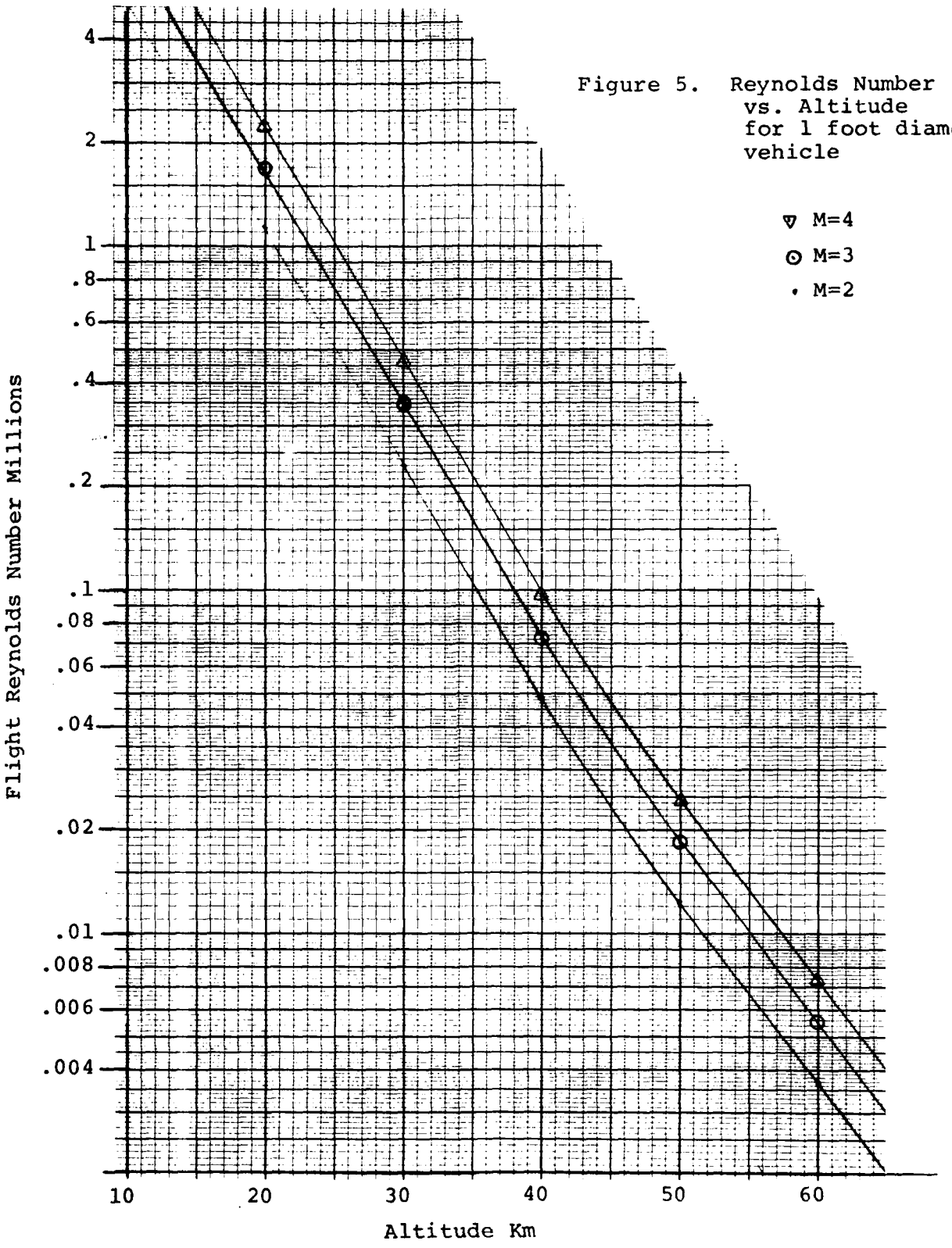

Figure 5. Reynolds Number vs. Altitude for 1 foot diameter vehicle

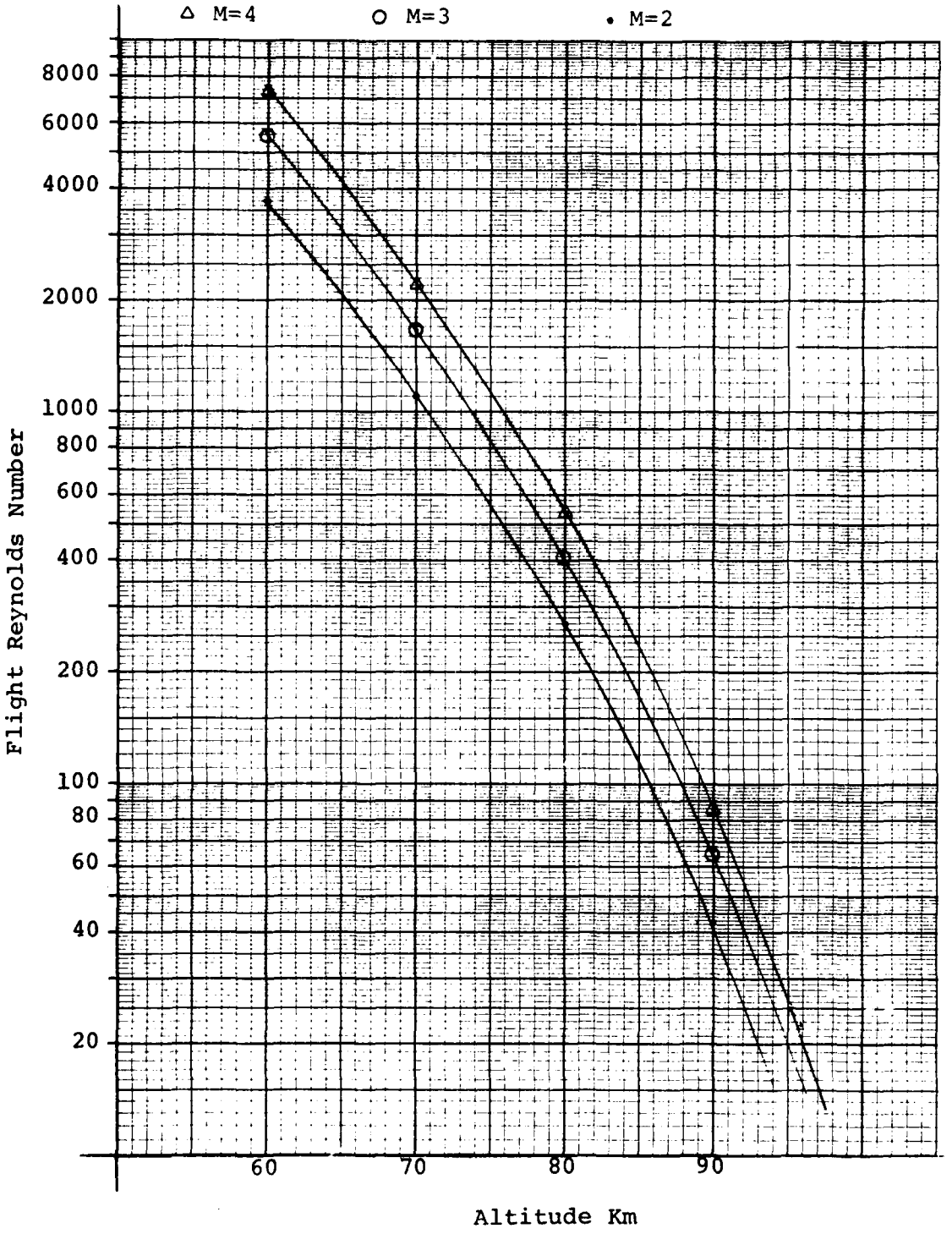

Figure 6. Reynolds Number vs. Altitude for 1 foot diameter vehicle

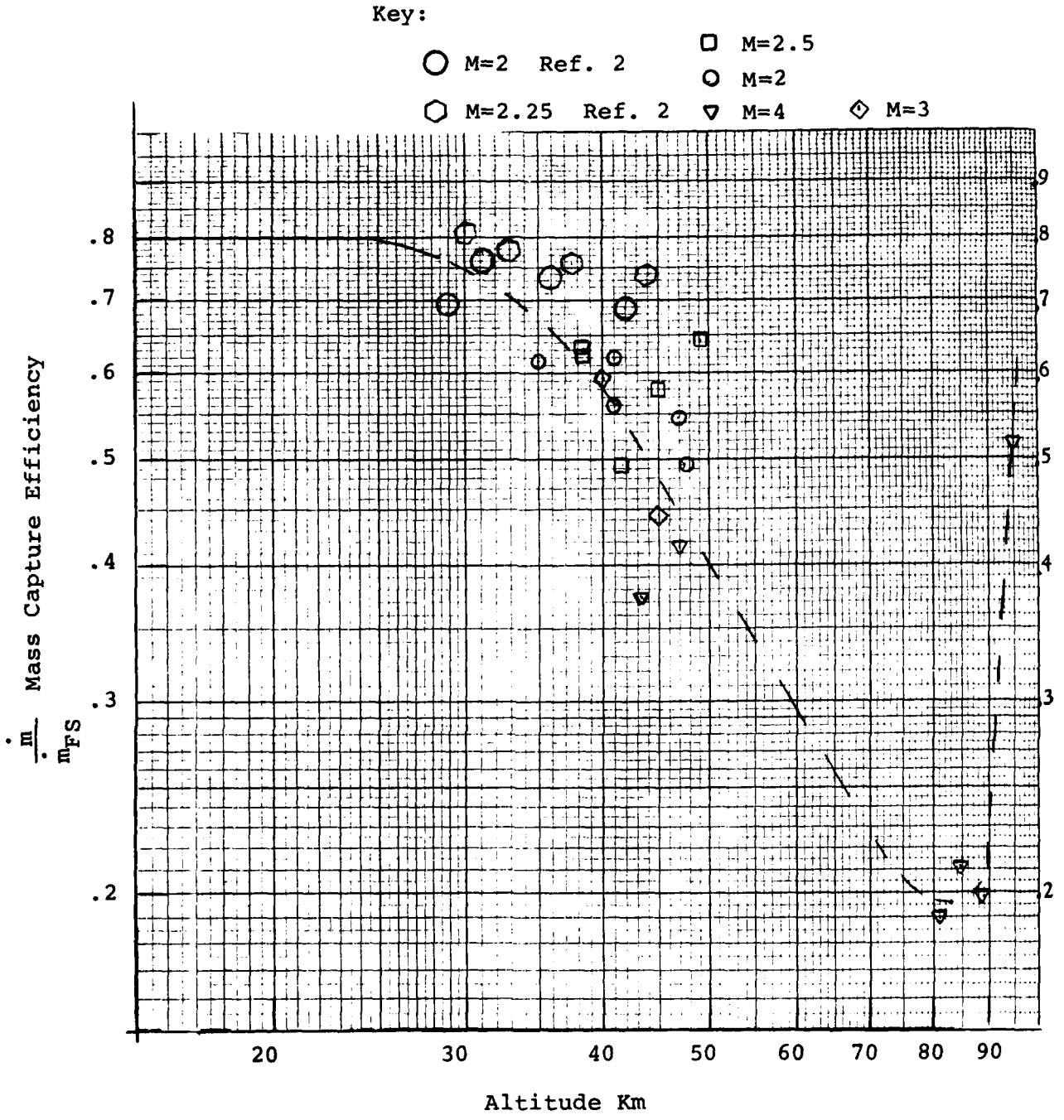

Figure 7. Mass Capture Efficiency vs. Altitude

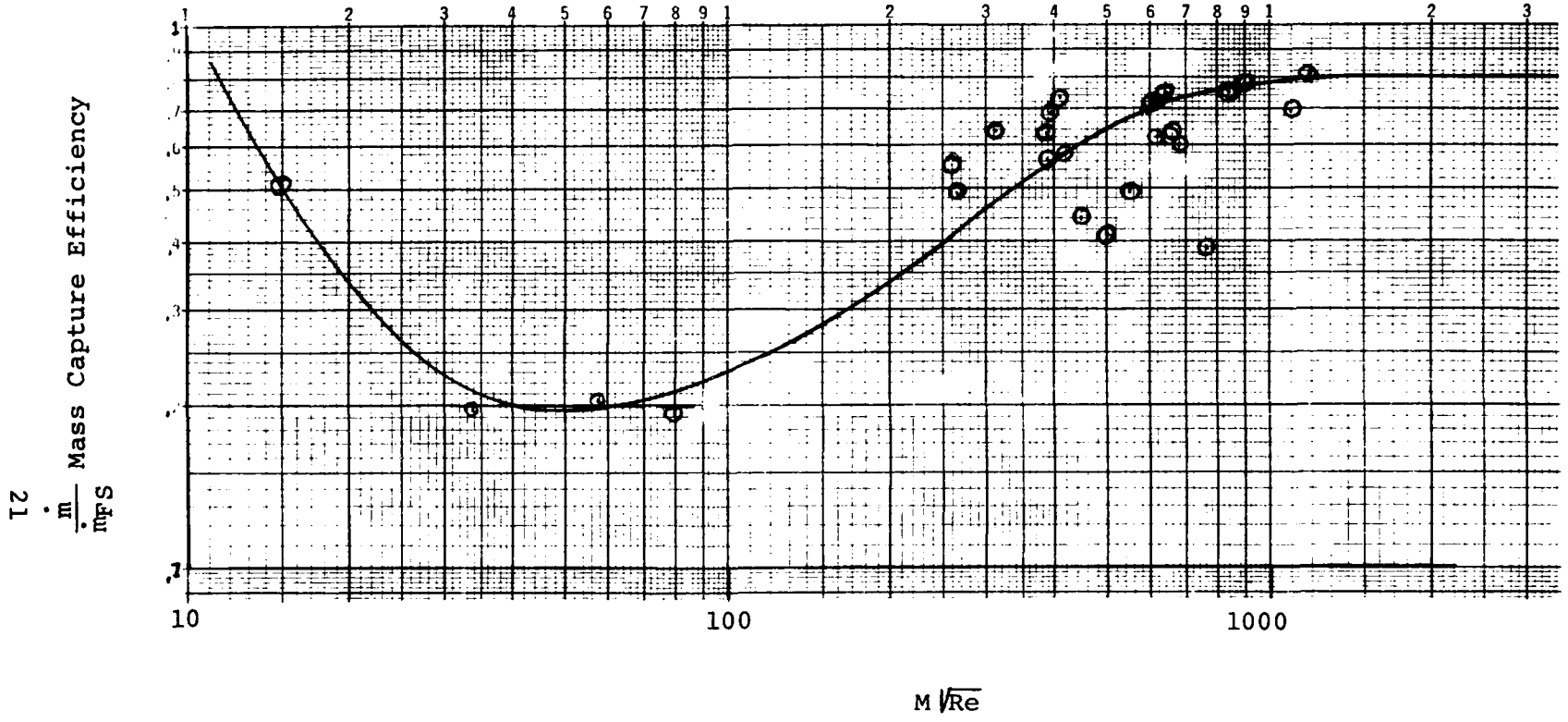

Figure 8. Mass Capture Efficiency
vs. Viscous Interaction Parameter

Figure 9. Attachment Boundary

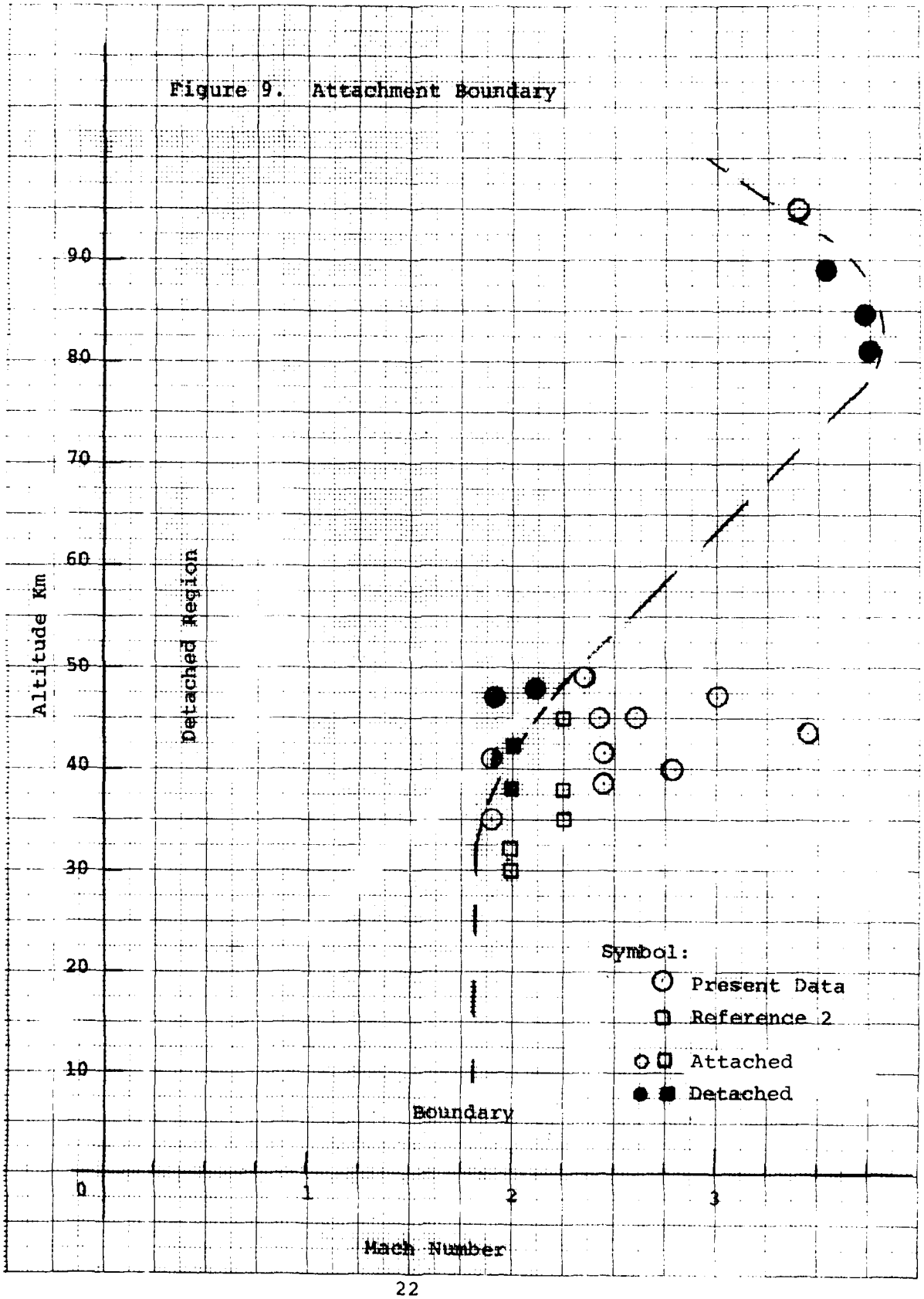

APPENDIX

Figures A-1 to A-8

Mach number and mass flux profiles from AEDC tests

Table A-1

Tabulated AEDC data with calculated Mach numbers and mass fluxes.

Key to Symbols on Figures A-1 to A-8

\+ 180° roll angle (side away from Gerdien)
13.2 inch station

⊙ 0° roll angle 13.2 inch station
(.2 inch ahead of Gerdien)

⊡ 0° roll angle 15.9 inch station
(.2 inch behind Gerdien)

◈ 4.4° roll angle -15.9 inch station
(offset from center of Gerdien)

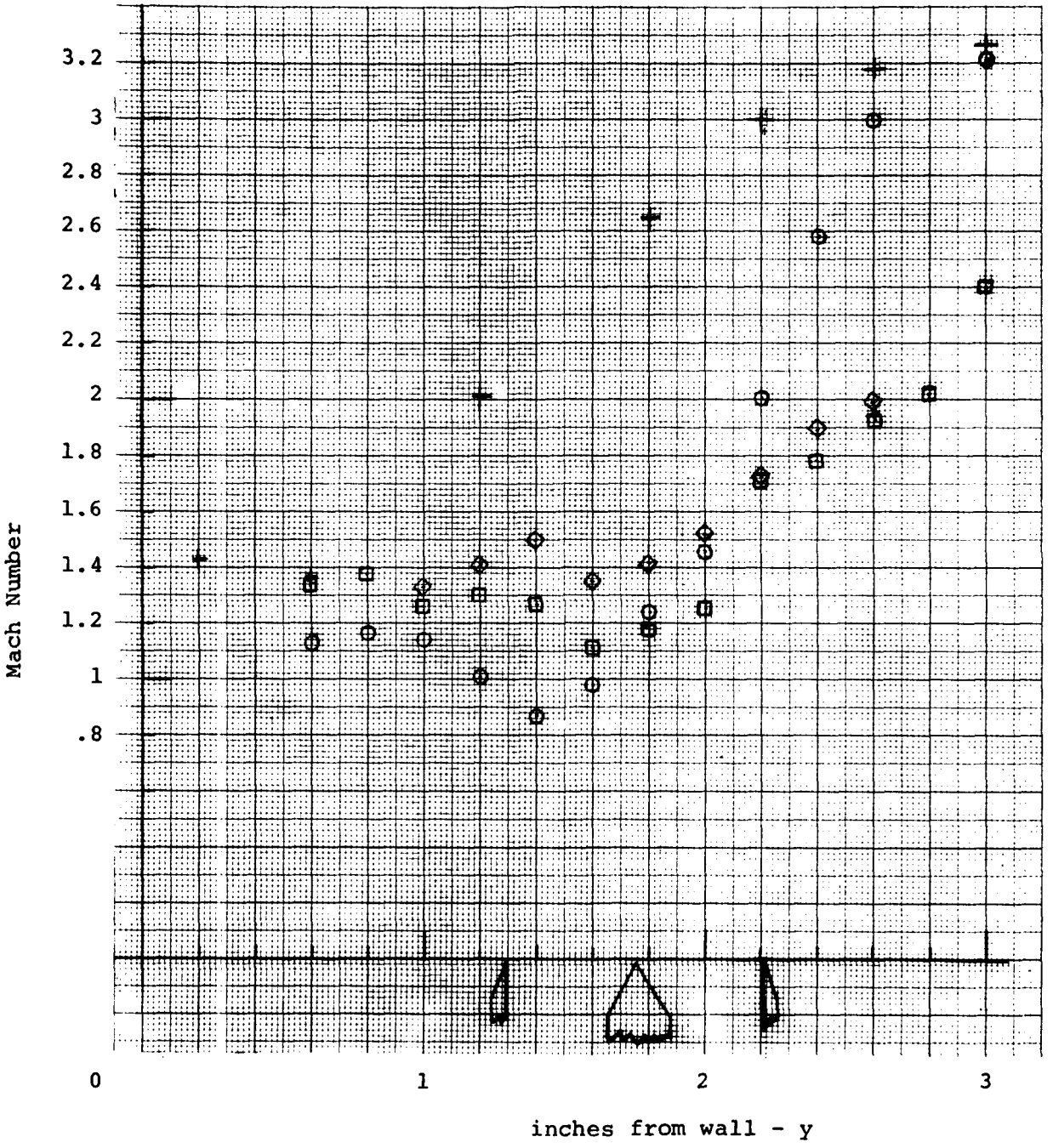

Figure A-1. Mach Number Profiles for Condition A 81 Km

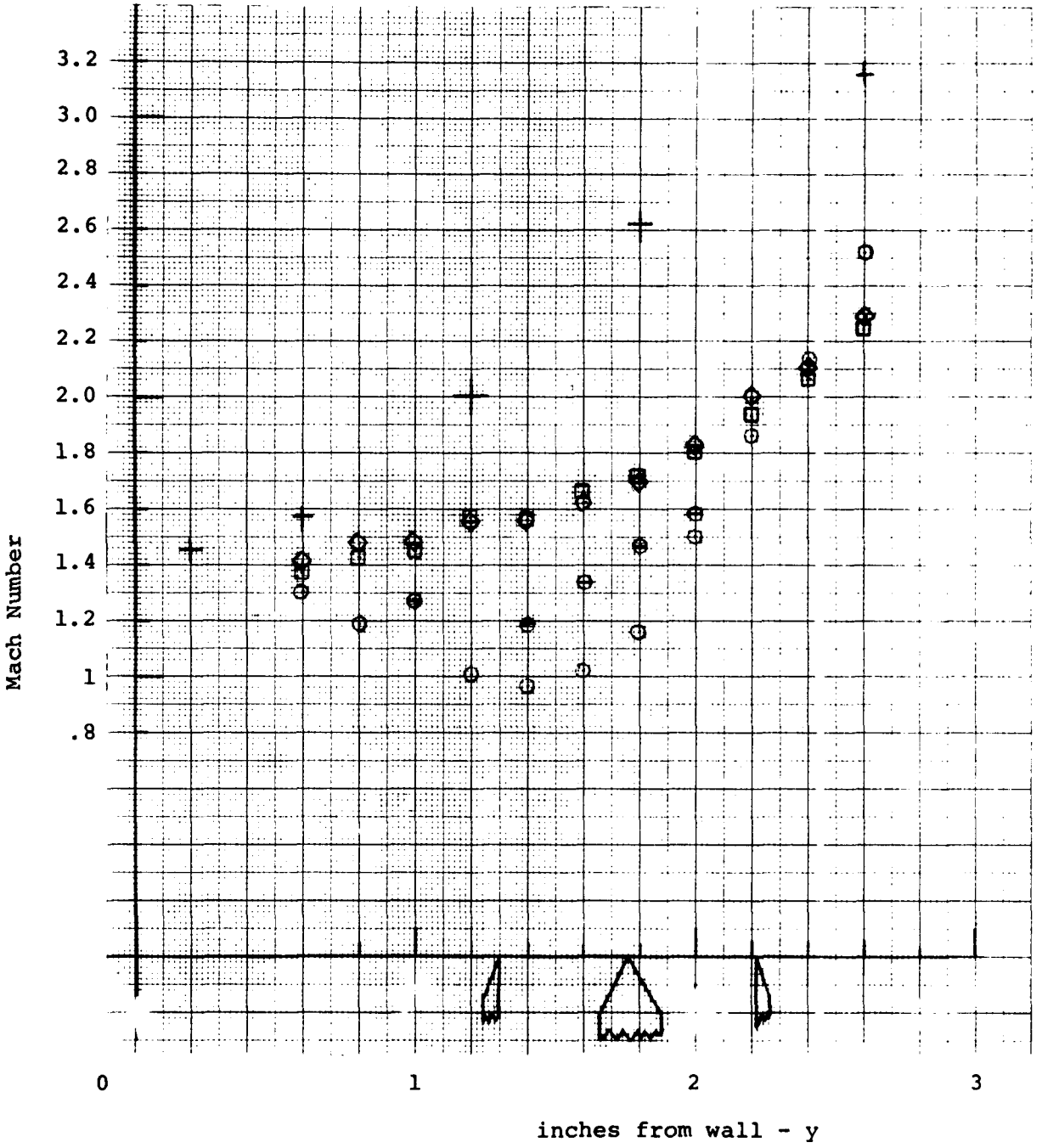

Figure A-2. Mach Number Profiles for Condition B 84.5 Km

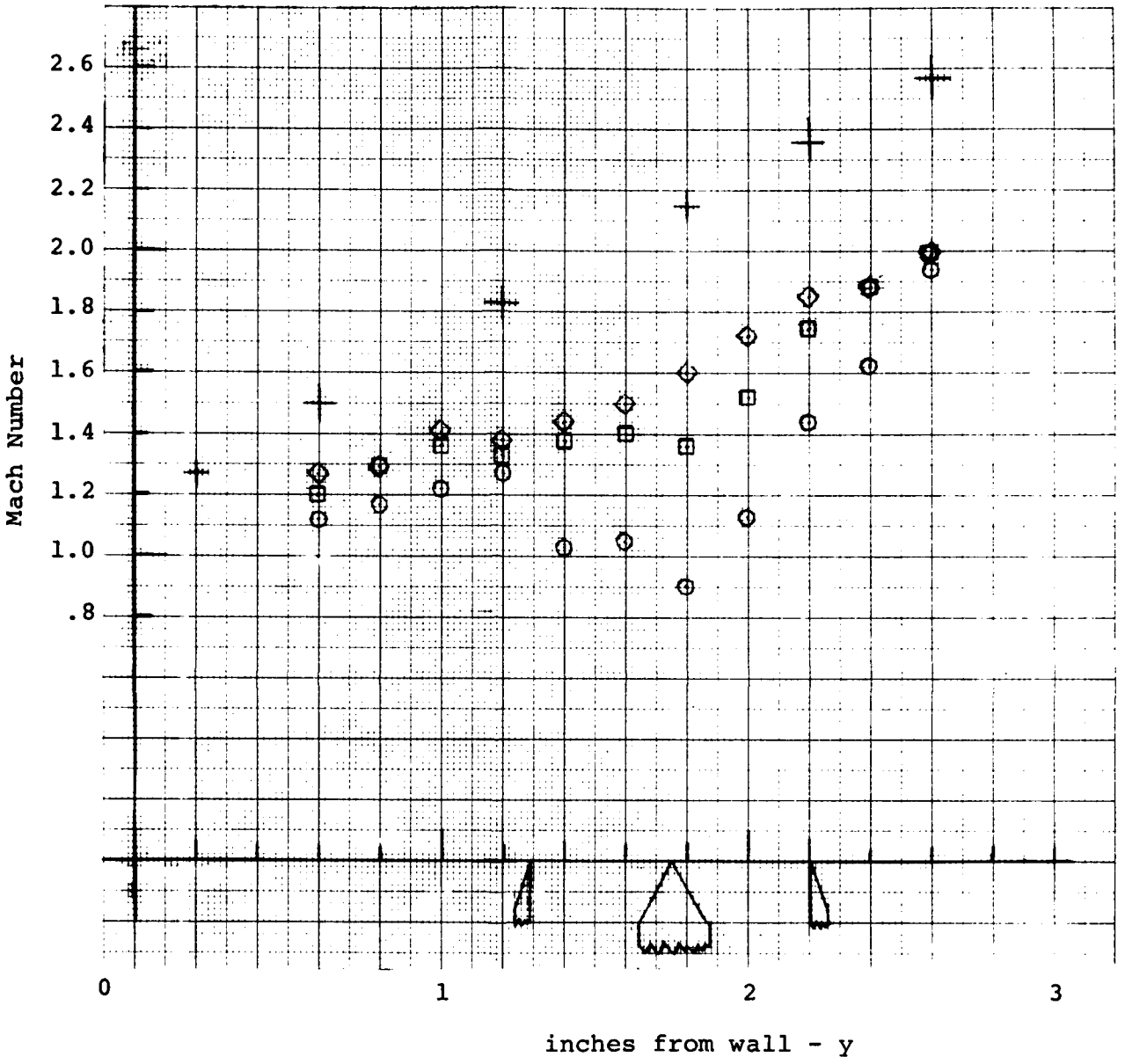

Figure A-3. Mach Number Profiles for Condition C 89 Km

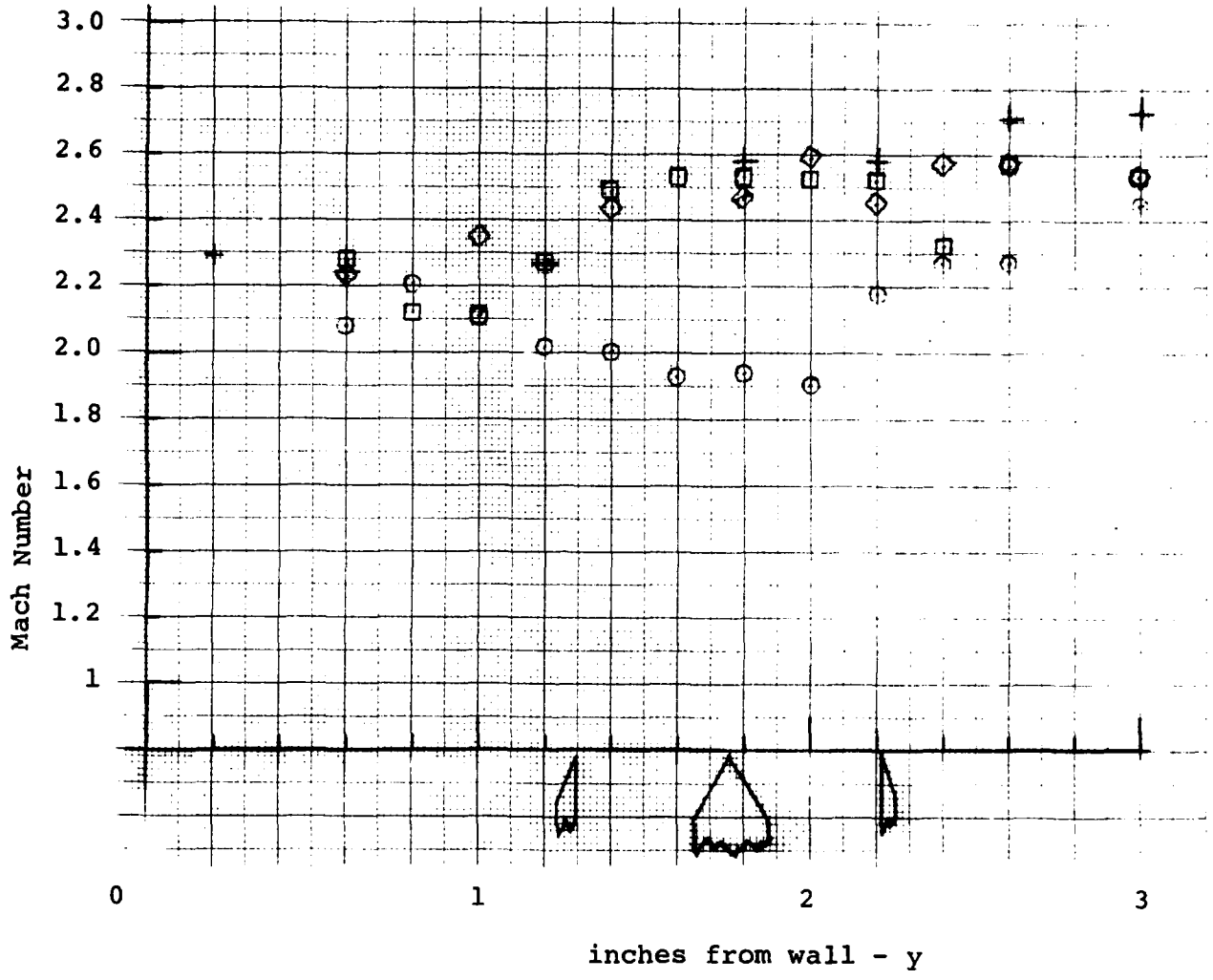

Figure A-4. Mach Number Profiles
for Condition D 95 Km

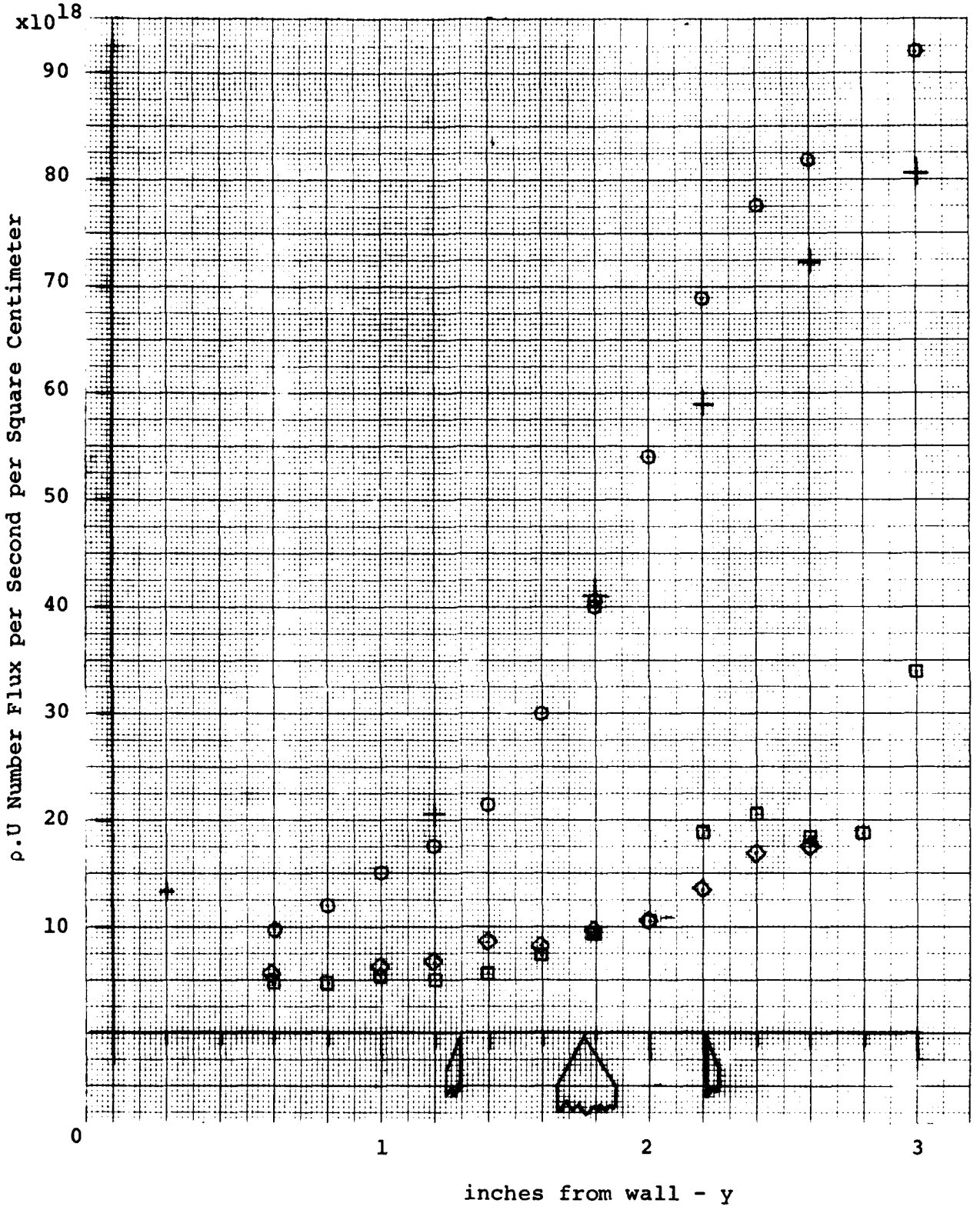

Figure A-5. Number Flux Profiles for Condition A 81 Km

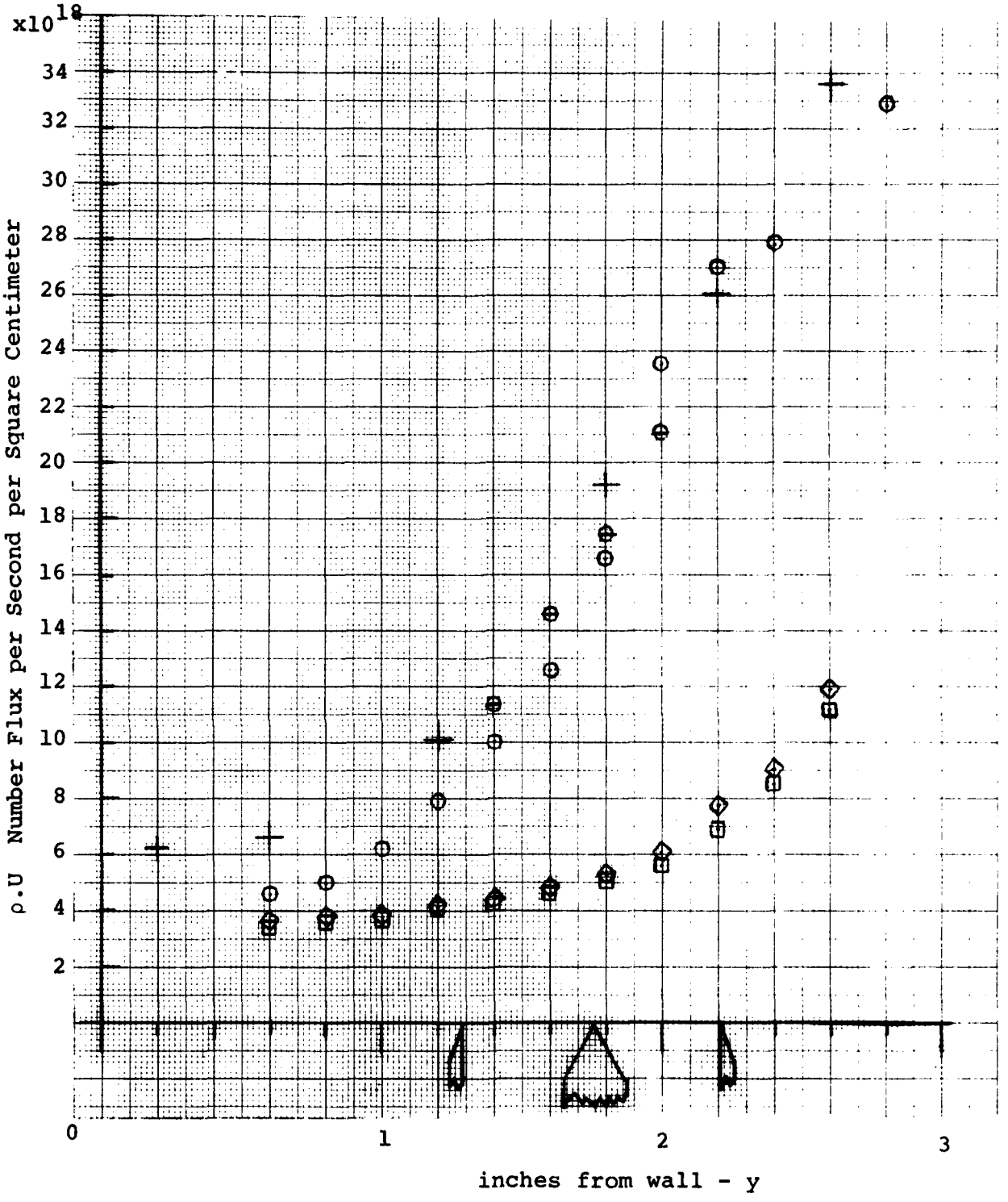

Figure A-6. Number Flux Profiles for Condition B 84.5 Km

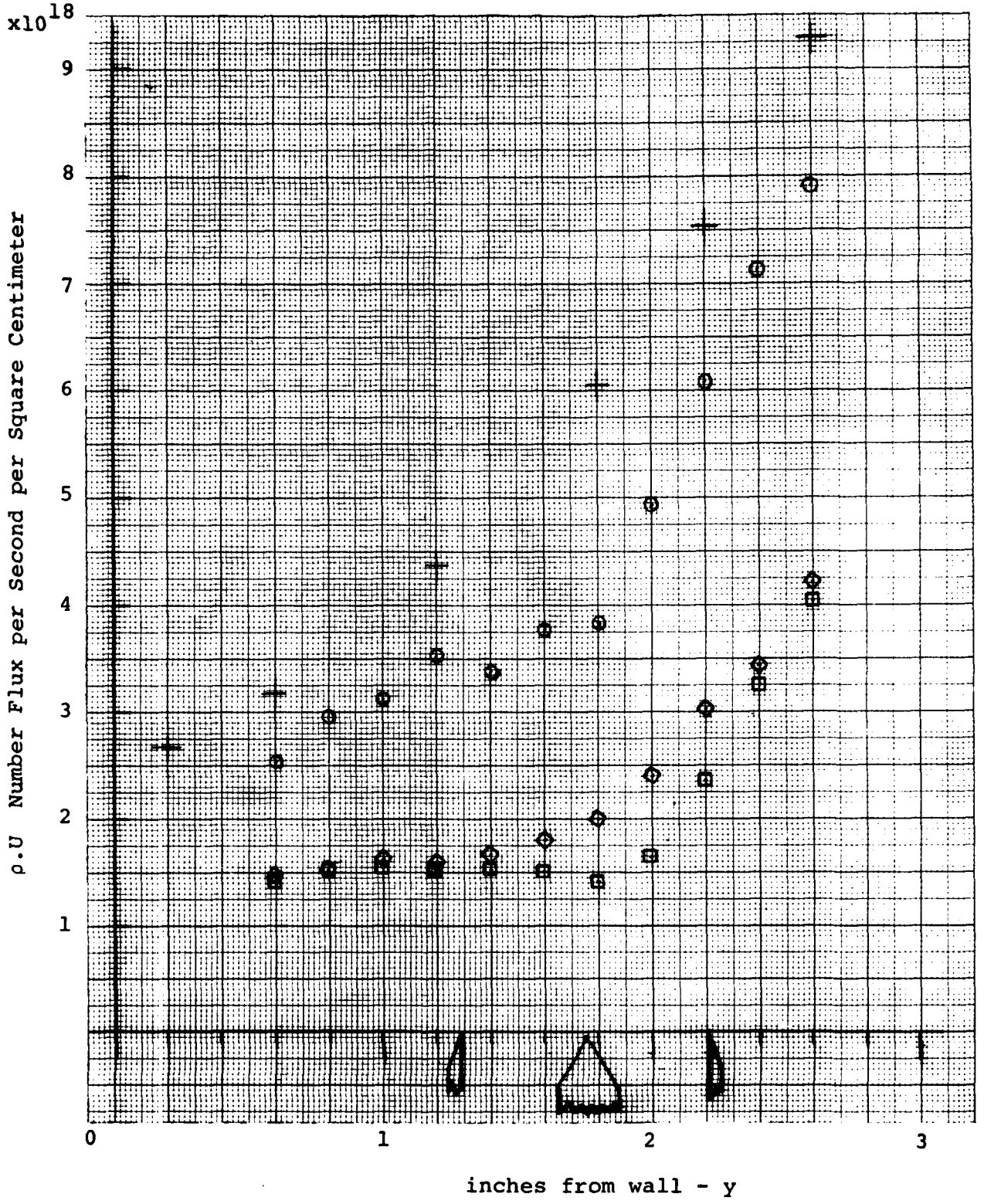

Figure A-7. Number Flux Profiles for Condition C 89 Km

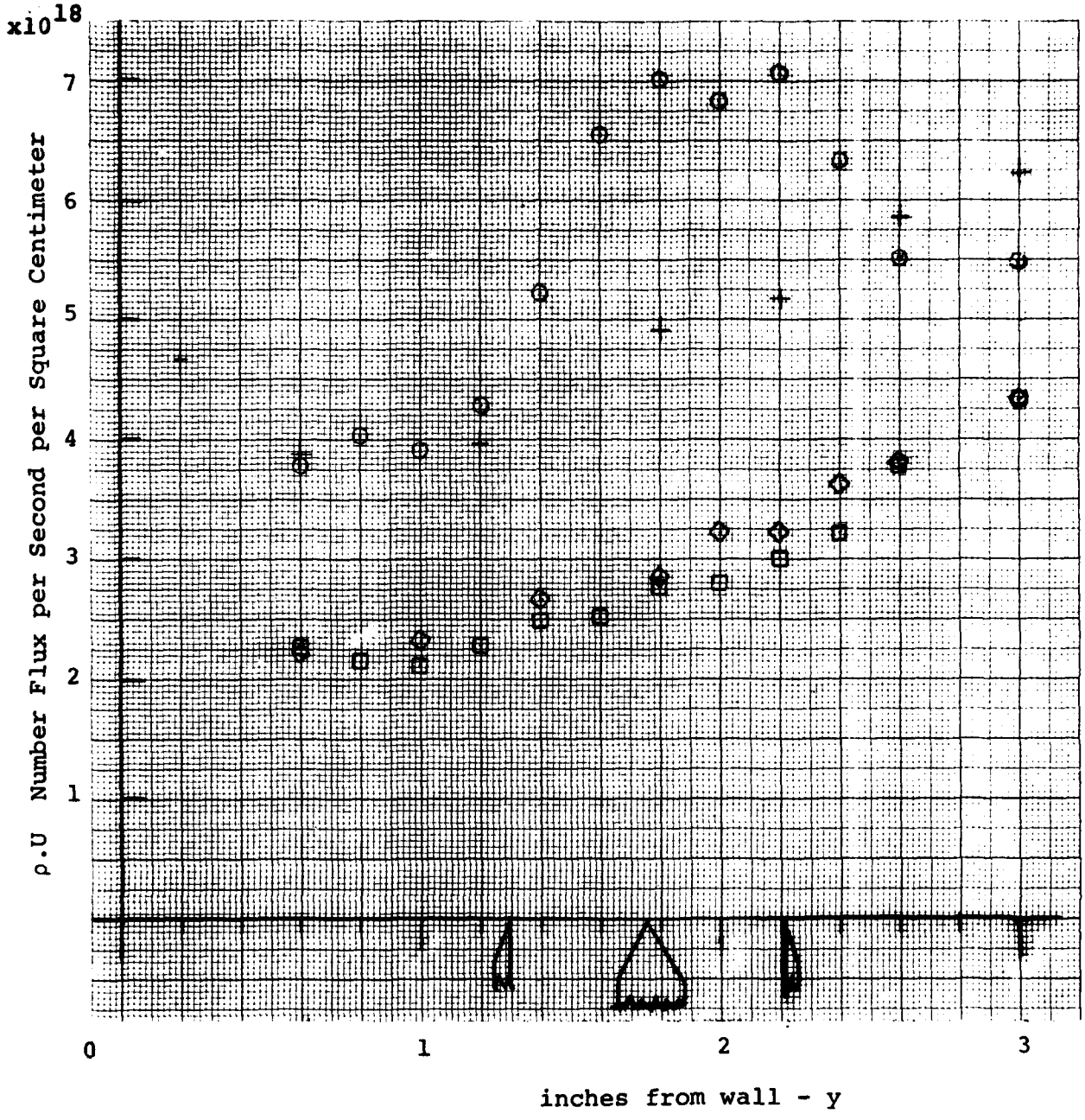

Figure A-8. Number Flux Profiles for Condition D 95 Km

Table A-1

AEDC Data (3) with calculated
Mach Number and Mass Fluxes

(Tunnel Condition C)

Θ	X(inch)	Y(inch)	T_R(K)	ρ(cm^{-3})	u(m/s)	M	ρu x 10^{-18} (N/cm^2/sec)
0°	0	0	93.8	2.21 E14			
			94.3	2.19 E14			
		5.49	79.8	2.21 E14			
			80.6	2.13 E14			
			80.8	2.08 E14			
			81.1	2.02 E14			
	Freestream		80.6	2.11 E14	647	3.54	13.65
0°	10.7	0.6	195.0	7.85 E13	425		
		0.8	184.8	8.41 E13	451		
		1.0	173.9	9.15 E13	474		
		1.2	164.2	9.94 E13	494		
		1.4	156.1	1.097 E14	511		
		1.6	149.4	1.219 E14	525		
		1.8	139.5	1.341 E14	544		
		2.0	132.2	1.484 E14	558		
		2.2	127.5	1.624 E14	566		
		2.4	122.0	1.792 E14	576		
		2.6	114.8	1.986 E14	589		
180°	10.7	0.2	212.0	7.15 E13	381	1.28	
		0.6	191.0	7.66 E13	434	1.54	
		1.2	165.8	9.62 E13	491	1.87	
		1.8	143.9	1.269 E14	535	2.19	
		2.2	127.8	1.585 E14	566	2.45	
		2.6	117.2	1.895 E14	585	2.65	
0°	13.2	0.6	225.1	7.36 E13	343	1.12	2.524
		0.8	220.8	8.30 E13	356	1.17	2.95
		1.0	217.0	8.78 E13	367	1.22	3.11
		1.2	213.1	9.32 E13	378	1.27	3.52
		1.4	232.3	1.053 E14	321	1.03	3.38
		1.6	230.6	1.159 E14	326	1.05	3.78
		1.8	242.6	1.340 E14	285	.90	3.82
		2.0	224.1	1.414 E14	347	1.13	4.91
		2.2	198.9	1.463 E14	415	1.44	6.07
		2.4	184.2	1.584 E14	450	1.63	7.13
		2.6	160.6	1.577 E14	502	1.94	7.92

Table A-1 (continued)

Tunnel Condition C

Θ	X(inch)	Y(inch)	T_R(K)	ρ(cm^{-3})	u(m/s)	M	ρu x 10^{-18} (N/cm^2/sec)
180°	13.2	0.2	213.0	7.09 E13	378	1.27	2.68
		0.6	194.0	7.42 E13	427	1.5	3.17
		1.2	168.8	9.04 E13	485	1.83	4.38
		1.8	146.2	1.143 E14	531	2.15	6.06
		2.2	133.0	1.357 E14	556	2.36	7.54
		2.6	121.3	1.608 E14	578	2.57	9.29
0°	15.9	0.6	218.6	3.89 E13	362	1.20	1.41
		0.8	211.3	3.96 E13	383	1.29	1.52
		1.0	206.2	3.91 E13	397	1.36	1.55
		1.2	208.2	3.92 E13	391	1.33	1.53
		1.4	204.4	3.81 E13	401	1.38	1.53
		1.6	202.1	3.69 E13	407	1.40	1.50
		1.8	205.5	3.51 E13	398	1.36	1.40
		2.0	192.7	3.81 E13	430	1.52	1.64
		2.2	174.9	5.02 E13	471	1.75	2.36
		2.4	165.0	6.59 E13	493	1.88	3.25
		2.6	156.9	7.93 E13	509	1.99	4.04
4.4°	15.9	0.6	213.4	3.92 E13	377	1.27	1.48
		0.8	211.3	3.97 E13	383	1.29	1.52
		1.0	201.9	4.00 E13	408	1.41	1.63
		1.2	204.5	4.02 E13	401	1.38	1.61
		1.4	199.4	4.07 E13	414	1.44	1.69
		1.6	194.4	4.22 E13	426	1.50	1.80
		1.8	186.5	4.49 E13	445	1.60	2.0
		2.0	177.0	5.17 E13	467	1.72	2.41
		2.2	166.9	6.18 E13	488	1.85	3.02
		2.4	165.0	6.98 E13	493	1.88	3.44
		2.6	154.0	8.18 E13	515	2.04	4.21
0°	17.7	0.6	216.1	4.42 E13	369		
		0.8	207.0	4.58 E13	394		
		1.0	197.0	4.73 E13	420		
		1.2	198.3	4.94 E13	417	1.45	
		1.4	191.7	5.22 E13	433	1.53	
		1.6	184.3	5.50 E13	450	1.62	
		1.8	178.4	5.84 E13	463	1.70	
		2.0	171.2	6.39 E13	480	1.8	
		2.2	163.0	6.86 E13	497	1.9	
		2.4	159.9	7.44 E13	504	1.95	
		2.6	151.3	8.29 E13	521		
180°	17.7	0.2	206.0	6.63 E13	397		
		0.6	192.0	6.95 E13	432		
		1.2	170.7	8.10 E13	481	1.80	
		1.8	149.6	1.004 E14	524	2.1	
		2.0	144.5	1.091 E14	535	2.18	
		2.6	127.3	1.373 E14	567	2.46	

Table A-1 (continued)

Tunnel Condition C

Θ	X(inch)	Y(inch)	T_R(K)	ρ(cm^{-3})	u(m/s)	M	ρu x 10^{-18} (N/cm^2/sec)
0°	4.0	1.8	119.6	3.039 E14	581	2.61	
	8.0		135.2	1.750 E14	552	2.32	
	9.0		137.8	1.534 E14	547	2.28	
	12.0		152.6	1.217 E14	519	2.06	
	12.7		184.3	1.266 E14	450	1.62	
	13.2		245.5	1.513 E14	275	.86	
180°	8.0	1.8	134.9	1.773 E14	553	2.33	
	12.0		144.8	1.260 E14	534	2.17	
	12.7		146.7	1.223 E14	530	2.14	

Tunnel Condition B

0°	0	5.49	81.5	5.12 E14			
			81.8	5.10 E14			
			79.9	5.12 E14			
	Freestream		81.1	5.11 E14	686		35.1
0°	10.7	0.6	197.8	1.55 E14	477		
		0.8	185.9	1.74 E14	503		
		1.0	170.1	2.02 E14	534		
		1.2	158.2	2.31 E14	557		
		1.4	146.2	2.71 E14	579		
		1.6	131.5	3.16 E14	605		
		1.8	122.1	3.74 E14	621		
		2.0	113.2	4.26 E14	635		
		2.2	106.1	4.92 E14	647		
		2.4	101.8	5.43 E14	654		
		2.6	98.6	5.91 E14	659		
180°	10.7	0.2	214.8	1.49 E14	441		
		0.6	197.1	1.50 E14	479		
		1.2	158.2	2.20 E14	557		
		1.8	126.0	3.52 E14	614		
		2.0	114.8	4.07 E14	633		
		2.6	99.9	5.75 E14	657		
0°	13.2	0.6	228.6	1.14 E14	405	1.31	4.62
		0.8	235.8	1.29 E14	386	1.19	4.98
		1.0	232.3	1.58 E14	395	1.27	6.24
		1.2	247.9	2.25 E14	352	1.09	7.92
		1.4	258.4	3.23 E14	319	.97	10.3
		1.6	254.5	3.81 E14	332	1.02	12.6
		1.8	242.2	4.50 E14	368	1.16	16.6
		2.0	211.8	5.27 E14	446	1.50	23.5
		2.2	181.2	5.27 E14	512	1.86	27.0
		2.4	160.9	5.04 E14	552	2.13	27.8
		2.6	135.4	5.49 E14	598	2.52	32.8

Table A-1 (continued)

Tunnel Condition B

Θ	X(inch)	Y(inch)	T_R(K)	ρ(cm^{-3})	u(m/s)	M	ρu x 10^{-18} (N/cm^2/sec)
180°	13.2	0.2	215.5	1.43 E14	437	1.46	6.24
		0.6	206.1	1.43 E14	459	1.57	6.56
		1.2	167.6	2.02 E14	539	2.04	10.9
		1.8	129.8	3.15 E14	608	2.62	19.2
		2.2	115.0	4.12 E14	633	2.90	26.1
		2.6	102.7	5.15 E14	652	3.16	33.6
0°	13.0	1.4	239.9	3.04 E14	375	1.19	11.4
		1.6	226.7	3.56 E14	410	1.34	14.6
		1.8	214.4	3.97 E14	440	1.47	17.5
		2.0	204.9	4.55 E14	462	1.58	21.0
	15.9	0.6	223.9	8.25 E13	417	1.37	3.44
		0.8	218.3	8.43 E13	430	1.43	3.62
		1.0	216.5	8.66 E13	435	1.45	3.76
		1.2	205.7	8.78 E13	460	1.57	4.04
		1.4	206.9	9.32 E13	457	1.56	4.25
		1.6	197.9	9.71 E13	477	1.66	4.63
		1.8	193.7	1.03 E14	486	1.71	5.01
		2.0	186.4	1.12 E14	502	1.80	5.62
		2.2	176.0	1.32 E14	523	1.93	6.90
		2.4	166.2	1.56 E14	542	2.06	8.46
		2.6	153.3	1.96 E14	566	2.24	11.1
4.4°	15.9	0.6	220.3	8.59 E13	426	1.41	3.66
		0.8	213.3	8.67 E13	442	1.48	3.83
		1.0	213.3	8.68 E13	442	1.48	3.84
		1.2	208.3	8.99 E13	454	1.54	4.08
		1.4	205.8	9.67 E13	460	1.57	4.45
		1.6	201.1	1.03 E14	470	1.63	4.84
		1.8	194.5	1.10 E14	484	1.70	5.32
		2.0	186.0	1.22 E14	502	1.81	6.12
		2.2	171.4	1.46 E14	532	1.99	7.77
		2.4	163.6	1.66 E14	547	2.10	9.08
		2.6	150.5	2.09 E14	571	2.28	11.9
0°	4.0	1.8	112.1	8.46 E14	637	2.95	
	6.0		115.6	7.03 E14	632	2.88	
	8.0		117.3	4.73 E14	629	2.85	
	9.0		120.5	4.18 E14	623	2.78	
	12.0		135.5	3.12 E14	598	2.52	
	12.8		226.5	3.96 E14	410	1.34	
	12.0	1.8	130.0	3.24 E14	607	2.61	
	13.0		135.7	2.97 E14	598	2.52	
	17.7		149.6	2.27 E14	573	2.3	

Table A-1 (continued)

Tunnel Condition D

Θ	X(inch)	Y(inch)	T_R(K)	ρ(cm^{-3})	u(m/s)	M	ρu x 10^{-18} ($N/cm^2/sec$)
0°	0	5.72	190.4	7.22 E13			
			205.7	6.66 E13			
			207.4	7.00 E13			
	Freestream		201.2	6.95 E13	988	3.42	6.87
0°	10.7	0.6	331.8	4.87 E13	840		
		0.8	325.4	4.67 E13	848		
		1.0	332.6	4.78 E13	839		
		1.2	306.4	5.11 E13	871		
		1.4	303.0	5.15 E13	875		
		1.6	318.1	5.17 E13	857		
		1.8	291.5	5.64 E13	888		
		2.0	291.6	5.71 E13	888		
		2.2	282.4	5.94 E13	959		
		2.4	271.2	6.24 E13	912		
		2.6	276.0	6.58 E13	906		
		3.0	266.7	6.91 E13	917		
180°	10.7	0.2	350.9	5.35 E13	816		
		0.6	330.2	4.47 E13	842		
		1.2	310.6	4.81 E13	866		
		1.8	295.0	5.44 E13	884		
		2.2	275.7	6.14 E13	907		
		2.6	254.7	6.88 E13	930		
		3.0	261.9	6.98 E13	922		
0°	13.2	0.6	359.3	4.71 E13	805	2.08	3.79
		0.8	339.4	4.86 E13	830	2.21	4.03
		1.0	355.3	4.83 E13	809	2.11	3.91
		1.2	364.1	5.38 E13	798	2.05	4.29
		1.4	370.9	6.62 E13	789	2.01	5.22
		1.6	384.1	8.49 E13	772	1.93	6.55
		1.8	381.5	9.04 E13	775	1.94	7.01
		2.0	387.4	8.92 E13	767	1.91	6.84
		2.2	343.7	8.58 E13	824	2.18	7.07
		2.4	330.4	7.51 E13	841	2.27	6.32
		2.6	329.6	6.54 E13	842	2.27	5.51
		3.0	304.8	6.30 E13	872	2.45	5.49
180°	13.2	0.2	327.8	5.55 E13	844	2.29	4.68
		0.6	334.2	4.64 E13	836	2.24	3.88
		1.2	329.9	4.71 E13	842	2.27	3.96
		1.8	288.0	5.51 E13	892	2.58	4.91
		2.2	288.2	5.80 E13	892	2.58	5.17
		2.6	271.6	6.44 E13	911	2.71	5.87
		3.0	269.7	6.81 E13	913	2.73	6.22

Table A-1 (continued)

Tunnel Condition D

Θ	X(inch)	Y(inch)	T_R(K)	ρ(cm^{-3})	u(m/s)	M	ρu x 10^{-18} (N/cm^2/sec)
0°	15.9	0.6	314.5	2.63 E13	861	2.38	2.26
		0.8	353.1	2.64 E13	813	2.12	2.15
		1.0	353.6	2.53 E13	812	2.11	2.05
		1.2	330.1	2.74 E13	841	2.27	2.30
		1.4	299.3	3.01 E13	879	2.49	2.65
		1.6	293.3	3.11 E13	886	2.53	2.76
		1.8	293.5	3.11 E13	886	2.53	2.76
		2.0	292.3	3.16 E13	886	2.54	2.80
		2.2	294.7	3.39 E13	884	2.52	3.00
		2.4	322.2	3.81 E13	851	2.32	3.24
		2.6	288.4	4.21 E13	892	2.57	3.76
		3.0	293.6	4.90 E13	885	2.53	4.34
4.4°	15.9	0.6	336.5	2.69 E13	834	2.23	2.24
		1.0	319.3	2.74 E13	855	2.35	2.34
		1.4	306.9	3.07 E13	870	2.44	2.67
		1.8	302.0	3.26 E13	875	2.47	2.85
		2.0	286.1	3.60 E13	894	2.59	3.22
		2.2	305.0	3.70 E13	872	2.45	3.23
		2.4	289.3	4.07 E13	890	2.57	3.62
		2.6	289.4	4.28 E13	890	2.57	3.81
		3.0	292.6	4.89 E13	887	2.54	4.34
0°	0	1.8	209.4	7.20 E13	979	3.32	
	2.0		243.5	1.071 E14	942	2.96	
	4.0		280.8	8.20 E13	900	2.64	
	6.0		280.1	8.23 E13	901	2.64	
	8.0		284.3	6.73 E13	896	2.61	
	9.0		288.5	6.37 E13	891	2.57	
	12.0		307.6	5.60 E13	869	2.43	
	12.5		315.2	5.91 E13	860	2.38	
	12.9		338.6	7.12 E13	831	2.22	
	18.0		313.7	3.30 E13	861	2.39	
180°	12.0	1.8	294.9	5.72 E13	884	2.53	
	15.0		299.2	5.11 E13	879	2.49	
	18.0		292.8	4.73 E13	886	2.54	

Tunnel Condition A

0°	0	5.72	82.7	9.93 E14			
			80.1	1.146 E15			
			80.4	9.70 E14			
			83.0	1.058 E15			
			84.9	1.032 E15			
	Freestream		82.2	1.04 E15	656		6.82

Table A-1 (continued)

Tunnel Condition A

θ	X(inch)	Y(inch)	T_R(K)	ρ(cm^{-3})	u(m/s)	M	ρu x 10^{-18} (N/cm^2/sec)
0°	10.7	0.6	195.2	2.78 E14	442	1.13	
		0.8	175.1	3.57 E14	487	1.81	
		1.0	163.8	3.82 E14	511		
		1.2	147.7	4.64 E14	542		
		1.4	130.6	5.76 E14	574		
		1.6	120.0	7.05 E14	593		
		1.8	111.5	8.11 E14	608		
		2.0	103.3	9.35 E14	622		
		2.2	99.0	1.047 E15	629		
		2.4	95.6	1.166 E15	634		
		2.6	95.7	1.191 E15	634		
		3.0	94.3	1.323 E15	637		
180°	10.7	0.2	207.4	3.14 E14	412		
		0.6	199.2	2.66 E14	432		
		1.2	149.5	4.44 E14	539		
		1.8	113.1	9.20 E14	605		
		2.2	101.7	1.170 E15	624		
		2.6	94.9	1.217 E15	636		
		3.0	94.6	1.314 E15	636		
0°	13.2	0.6	230.3	2.81 E14	350	1.13	9.84
		0.8	227.5	3.36 E14	358	1.16	12.0
		1.0	229.6	4.26 E14	352	1.14	15.0
		1.2	240.3	5.48 E14	319	1.01	17.5
		1.4	251.0	7.65 E14	281	.87	21.5
		1.6	242.6	9.64 E14	311	.98	30.0
		1.8	221.5	1.089 E15	375	1.24	40.8
		1.8	226.4	1.115 E15	361	1.18	40.2
		2.0	203.7	1.283 E15	421	1.45	54.0
		2.2	160.7	1.333 E15	517	2.0	68.9
		2.4	123.9	1.319 E15	586	2.58	77.3
		2.6	105.7	1.323 E15	618	2.95	81.8
		3.0	94.6	1.446 E15	636	3.21	92.0
180°	13.2	0.2	207.5	3.17 E14	419	1.43	13.3
		0.6	210.2	2.51 E14	405	1.37	10.2
		1.2	160.3	3.97 E14	518	2.01	20.6
		1.8	120.3	7.06 E14	592	2.65	41.8
		2.2	103.5	9.47 E14	622	3.0	58.9
		2.6	95.9	1.139 E15	634	3.18	72.2
		3.0	92.2	1.260 E15	640	3.27	80.6

Table A-1 (continued)

Tunnel Condition A

θ	X(inch)	Y(inch)	T_R(K)	ρ(cm^{-3})	u(m/s)	M	ρu x 10^{-18} (N/cm^2/sec)
0°	15.9	0.6	228.7	1.36 E14	354	1.15	4.81
		0.8	226.6	1.34 E14	361	1.18	4.84
		1.0	219.3	1.37 E14	381	1.26	5.22
		1.2	216.0	1.33 E14	390	1.30	5.18
		1.4	218.5	1.47 E14	383	1.27	5.63
		1.6	232.0	2.12 E14	345	1.11	7.31
		1.8	226.4	2.54 E14	361	1.18	9.17
		2.0	220.4	2.78 E14	378	1.25	10.5
		2.2	182.4	3.98 E14	471	1.71	18.7
		2.2	177.3	4.20 E14	482	1.78	20.2
		2.4	165.6	3.63 E14	507	1.93	18.4
		2.6	159.7	3.65 E14	519	2.02	18.9
		3.0	134.7	5.99 E14	567	2.40	34.0
4.4°	15.9	1.0	213.3	1.55 E14	397	1.33	6.15
		1.2	206.8	1.61 E14	414	1.41	6.67
		1.4	199.9	2.01 E14	431	1.50	8.66
		1.6	211.9	2.10 E14	401	1.35	8.42
		1.8	206.2	2.34 E14	415	1.42	9.71
		2.0	198.2	2.54 E14	435	1.52	11.0
		2.2	181.8	2.83 E14	472	1.72	13.4
		2.4	168.3	3.38 E14	501	1.89	16.9
		2.6	161.6	3.39 E14	515	1.99	17.5
0°	0	1.8	80.1	1.085 E15	659	3.61	
	1.0		83.8	1.057 E15	653	3.50	
	2.0		82.1	2.103 E15	656*	3.55	
	2.0		88.1	1.567 E15	647**	3.38	
	4.0		108.3	1.608 E15	613	2.89	
	6.0		112.6	1.570 E15	606	2.80	
	8.0		108.1	1.176 E15	614	2.90	
	9.0		107.0	1.103 E15	615	2.92	
	12.0		110.7	1.074 E15	609*	2.84	
	12.0		112.6	7.86 E14	606**	2.80	
	12.5		117.4	6.93 E14	598	2.71	
	12.9		126.8	6.97 E14	581	2.53	
	13.0		167.6	6.53 E14	503	1.91	
	13.2		241.7	7.74 E14	314*	.99	
	18.0		180.4	2.29 E14	475	1.74	
180°	0	1.8	81.9	1.059 E15	656	3.56	
	2.0		83.6	1.592 E15	654	3.51	
	2.0		87.9	1.561 E15	647**	3.39	
	6.0		108.8	1.799 E15	612*	2.88	
	6.0		108.7	1.623 E15	612**	2.88	

Table A-1 (continued)

Tunnel Condition A

Θ	X(inch)	Y(inch)	T_R(K)	ρ(cm^{-3})	u(m/s)	M	ρu x 10^{-18} (N/cm^2/sec)
180°	8.0	1.8	106.0	1.589 E15	617*	2.94	
	8.0		106.0	1.239 E15	617**	2.94	
	9.0		90.9	2.510 E15	642*	3.30	
	9.0		106.9	1.070 E15	616**	2.92	
	12.0		108.8	8.61 E14	612	2.88	
	18.0		128.5	5.62 E14	578	2.50	

*Inconsistent Data -
Number Densities and some Temperatures not Plotted.

**Repeat Point